

Mixing Flows on the Torus

Craig Chen

December 13, 2021

Abstract

We study the mixing properties of a Lipschitz vector field on the torus \mathbb{T}^2 . This study is largely motivated by Bressan's conjecture on mixing flows; we will dedicate a section towards discussing this conjecture and progress towards its resolution. There are many perspectives from which one can study mixing - we focus on the dynamical systems approach.

1 Introduction

Mixing is a concept that is important in the disciplines of science and engineering. In applications, we are often interested in how to quantify the degree of homogenization of a substance under stirring and the rate at which this occurs. Of equal interest, though, are the properties of the stirring vector fields themselves. We are specifically interested in *non-diffusive* mixing of an incompressible fluid (*e.g.*, water). In this case, the mixing process can be modelled by the transport equation

$$\partial_t \varrho + f \cdot \nabla \varrho = 0, \quad (1.1)$$

where ϱ is a scalar function that can be thought of the concentration of some quantity being mixed and f as the fluid velocity. Incompressibility of the fluid requires f to be divergence-free (which follows from a conservation of mass argument). In the rest of this paper and many others, we will assume that ϱ is mean-zero (*i.e.*, $\int_{\Omega} \varrho(x, 0) dx = 0$ where Ω is the domain) as it makes computations much easier (and the transport equation is not affected by shifts). A special case we're also interested in is where $\varrho(\cdot, 0)$ is an indicator function minus some normalization constant which can be thought of as modeling the mixing of two fluids.

Overview: In the remainder of this section, we provide a brief introduction to different ways to quantify mixing as well as an overview of the connection between mixing and dynamical systems. In Section 2, we outline the conjecture which inspired this project as well as selected works that have come close to resolving this conjecture. We also introduce a “dual” problem which studies the properties of mixing vector fields, which we will focus on for the remainder of the paper. Of particular interest is the regularity of these mixing flows. In section 3 we introduce a family of Lipschitz vector fields and present various plots of mixing and the trajectory of points under these flows. In Section 4, we study the mixing properties of this family of vector fields — in particular, we explore a potential avenue for proving exponential mixing. The discussion and conclusion are in section 5.

1.1 Preliminaries and Background

We assume the reader is familiar with the basics of real analysis (*e.g.*, L^p spaces, measurability) and vector calculus (*e.g.*, relationships between common differential operators such as ∇ , div). We also assume the reader has heard of Sobolev spaces before - we do not need any detailed theoretical results about these spaces, rather, we only need to know the definition of their norms.

Notation: Unless explicitly specified, μ will always denote the Lebesgue measure. As shorthand, we denote by $f_A f = \mu(A)^{-1} \int_A f$ the average of f on A . We say $A \ll B$ if there exists some constant C independent of A, B . Similarly, $f = O(g)$ if $\exists x_0$ such that $\|f(x)\| \ll g(x)$ for all $x \geq x_0$.

Definition 1.1. The Sobolev space $H^k(\mathbb{T}^d)$ for $k \in \mathbb{Z}$ is defined as the space of square-integrable functions on the d -dimensional torus that satisfy

$$\|f\|_{H^k}^2 := \sum_{n=-\infty}^{\infty} (1 + |n|^2)^k |\hat{f}(n)|^2 < \infty.$$

Classical results show that H^k is a Hilbert space with inner product defined in terms of the L^2 inner product.

$$\langle u, v \rangle_{H^k} = \sum_{l=0}^k \langle D^l u, D^l v \rangle_{L^2}.$$

Also useful for us will be the homogeneous space \dot{H}^k with seminorm

$$\|f\|_{\dot{H}^k}^2 = \sum_{n=-\infty}^{\infty} |n|^{2k} |\hat{f}(n)|^2 = \|\nabla f\|_{L^2}. \quad (1.2)$$

By restricting to mean-zero functions, $\|\cdot\|_{\dot{H}^k}$ becomes a true norm. The details regarding the definition of the homogeneous space are not important for our use case (which is to study mixing). As we will see in the next section, there are many ways to measure mixing, and the negative Sobolev norms turn out to be one such method.

1.2 Measures of Mixing

In order to study mixing, we first need to define quantitatively what it means for an advected scalar ϱ to be mixed to some scale.

In the classical setting, a transformation $f : X \rightarrow X$ is said to be mixing if for any two measurable sets $A, B \subset X$,

$$\mu(A \cap f^{-n}(B)) \rightarrow \mu(A)\mu(B), \quad (1.3)$$

as $n \rightarrow \infty$. Another way to study how well such a map mixes is to look at correlations between observables on the domain. An observable is a real-valued, square-integrable function on X ; we often work with observables because in applications we can rarely monitor the actual states $x \in X$. For example, the indicator function of a set $A \subset X$ is an observable. Intuitively, if a map mixes effectively, a deterministic system may appear random after many timesteps.

Definition 1.2. For any $f, g \in L^2(X)$ and a discrete-time transformation of the space $T : X \rightarrow X$, we define the correlation function

$$C_{f,g}(n) = \int_X f(x)g(T^n(x)) dx - \int_X f(x)dx \int_X g(x)dx. \quad (1.4)$$

We note that these are technically covariances, although we can normalize f, g without consequence. Furthermore, rather than limiting ourselves to square-integrable functions, we can define this for pairs of functions that live in L^p and L^q where $\frac{1}{p} + \frac{1}{q} = 1$ for $1 \leq p, q \leq \infty$.

For an advected scalar, following the naming convention of [Thi12], we present the two quantitative definitions which have been the primary measures of mixing in recent years.

Definition 1.3. For $f \in L^\infty(X)$ such that $\int_X f = 0$ (*i.e.*, mean-zero), we define the following measures of mixing:

- (i) *Geometric mixing scale*: For $\kappa \in (0, 1/2)$, f is κ -mixed to scale $\varepsilon > 0$ if for every $y \in X$,

$$\left| \mathfrak{f}_{B(y,\varepsilon)} f(x) dx \right| \leq \kappa \|f\|_\infty.$$

- (ii) *Functional mixing scale*: For $q > 0$, the functional mixing scale of f is defined as

$$\|f\|_{\dot{H}^{-q}} \|f\|_\infty^{-1/q}.$$

Most commonly, $q = \frac{1}{2}, 1$.

There is a third definition which has also been used - the so-called Mix-Norm [MMP05].

$$\Phi(f) = \left(\int_{X \times (0,1)} \left(\mathfrak{f}_{B(y,r)} f(x) dx \right)^2 dy dr \right)^{\frac{1}{2}}$$

Naturally, one may wonder whether any of these definitions of mixing are equivalent. In [LLN⁺12], they show that the geometric and H^{-1} functional mixing scales are *not* equivalent. Equation (30) in [MMP05] shows that the Mix-Norm and $H^{-1/2}$ norms are equivalent for mean-zero functions. It is also quick to show that being κ -mixed to ε -scale implies mixing in the sense of the Mix-Norm

Lemma 1.4. Suppose $\mu(X) < \infty$. If f is κ -mixed to scale ε , then $\Phi(f) \ll \sqrt{\varepsilon + \kappa^2} \|f\|_\infty$.

Proof. We can write the mix-norm as follows.

$$\begin{aligned} \Phi(f)^2 &= \int_0^1 \int_X \left(\mathfrak{f}_{B(y,r)} f(x) dx \right)^2 dy dr \\ &= \int_0^\varepsilon \int_X \left(\mathfrak{f}_{B(y,r)} f(x) dx \right)^2 dy dr + \int_\varepsilon^1 \int_X \left(\mathfrak{f}_{B(y,r)} f(x) dx \right)^2 dy dr \\ &=: (1) + (2) \end{aligned}$$

We will now show that we can bound (1) by $\varepsilon \|f\|_\infty^2$ and (2) by $\kappa^2 \|f\|_\infty^2$. For (1), we notice that we can bound the average of the function in a ball by the maximum of the function, and we get that

$$\begin{aligned} (1) &= \int_0^\varepsilon \int_X \left(\mu(B(y, r))^{-1} \int_{B(y, r)} f(x) dx \right)^2 dy dr \\ &\leq \int_0^\varepsilon \int_X \|f\|_\infty^2 dy dr \\ &\ll \varepsilon \|f\|_\infty^2. \end{aligned}$$

For (2), we will use the assumed mixed-ness of f . Notice that for $r > \varepsilon$, we can cover $B(y, r)$ with a finite number of ε -balls. Explicitly, we will need order $\frac{r^d}{\varepsilon^d}$ balls. For each $y \in X$, let $U(y)$ denote such a covering. Then,

$$\begin{aligned} \int_{B(y, r)} f(x) dx &\leq \mu(B(y, r))^{-1} \sum_{u \in U(y)} \int_u f(x) dx \\ &\leq C \mu(B(y, r))^{-1} \frac{r^d}{\varepsilon^d} \mu(B(y, \varepsilon)) \kappa \|f\|_\infty \\ &\ll \kappa \|f\|_\infty, \end{aligned}$$

since the volume of a ball of radius r in \mathbb{R}^d is order r^d . This implies that

$$(2) \ll \kappa^2 \|f\|_\infty^2$$

which proves the claim. □

So far, we have studied the equivalence between quantitative definitions of mixing that only depend on a scalar function. However, recently it has been shown that there is a further connection between these mix-norms and the dynamical systems perspective of the decay of correlations. In [OTD20], they show that the mix-norm is the sharpest rate of decay of correlations in both the uniform sense and the asymptotic sense for observables $g \in \dot{H}^q$ ($q > 0$).

Before moving on, we mention a final result which highlights a difference between mixing with and without diffusion. Related to the above methods of measuring mixing, another rather natural candidate is the variance of the advected scalar function. However, as we will soon see, the variance is preserved by the transport equation (1.1). Assuming periodic boundary conditions, using integration by parts, we can calculate,

$$\begin{aligned} \frac{d}{dt} \int_\Omega \varrho^2 d\mu &= 2 \int_\Omega \varrho \partial_t \varrho d\mu \\ &= 2 \int_\Omega \varrho (-f \cdot \nabla \varrho) d\mu \\ &= \int_\Omega -f \cdot \nabla (\varrho^2) d\mu \\ &= \int_\Omega (\nabla \cdot u) \varrho^2 d\mu \end{aligned}$$

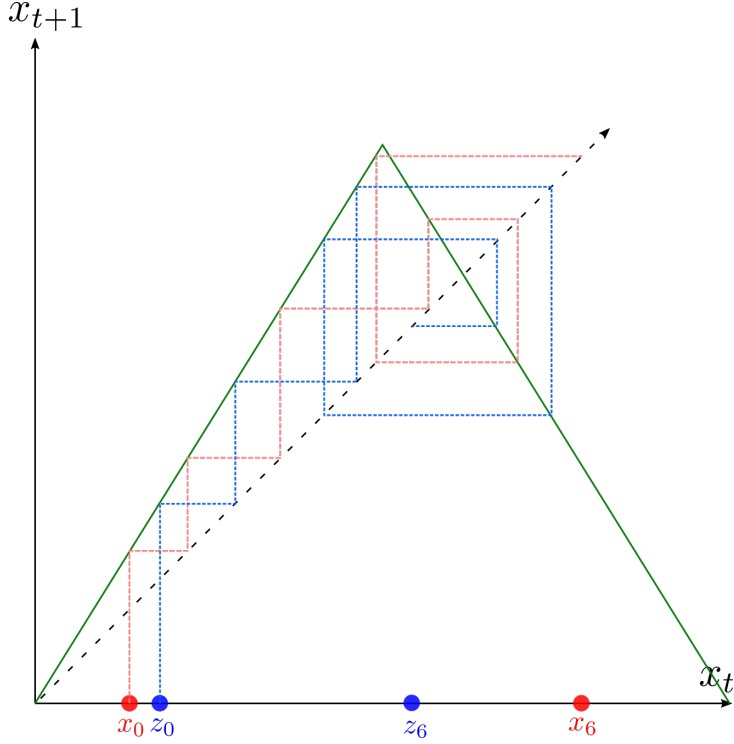


Figure 1: Cobweb diagram of the tent map. Notice how the points x_0 and z_0 start off close together but quickly separate.

which vanishes since u is a divergence-free vector field. Thus,

$$\frac{d}{dt} \|\varrho\|_{L^2}^2 = 0. \quad (1.5)$$

1.3 Dynamical Systems

The study of mixing flows is closely related to that of dynamical systems. We first provide an example.

Definition 1.5. The *tent map* is a map from $[0, 1]$ to $[0, 1]$ defined as

$$\Lambda(x) = \begin{cases} 2x & \text{if } x \leq \frac{1}{2} \\ 2 - 2x & \text{if } x > \frac{1}{2} \end{cases}$$

The tent map is a classic example of a map that produces *chaotic* dynamics under successive iterations. An intuitive definition of a chaotic system is one in which small changes to the initial condition produce wildly different outcomes - for reasons like these chaotic dynamical systems have even been used as random number generators! Figure 1 depicts an example trajectory of a point. When studying the mixing properties of vector fields, we can often view them from the perspective of a discrete-time dynamical system by following the destiny of some subset of the domain at integer time values. For example, the vector field defined by the alternating horizontal and vertical shears (see Figure 2

$$A(x, y, t) = \begin{cases} F(x, y) = (y, 0) & \text{if } t \in [2n, 2n + 1) \\ G(x, y) = (0, x) & \text{if } t \in [2n - 1, 2n) \end{cases}$$

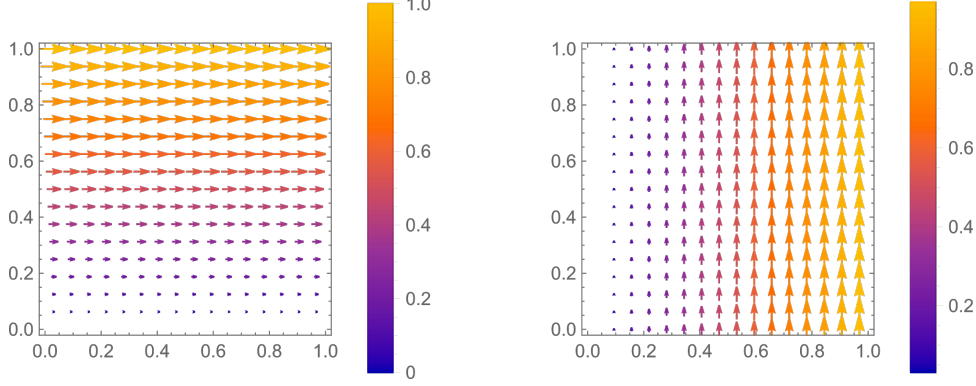


Figure 2: The alternating shears of the cat map.

produces a map known as *Arnold's cat map*. This is an example of a map that can be written as a flow as well - in general this may not be the case.

Definition 1.6. *Arnold's cat map* is an map from $\mathbb{T}^2 \rightarrow \mathbb{T}^2$, defined

$$\begin{bmatrix} x_{t+1} \\ y_{t+1} \end{bmatrix} = \begin{bmatrix} 2 & 1 \\ 1 & 1 \end{bmatrix} \begin{bmatrix} x_t \\ y_t \end{bmatrix} \mod 1$$

It is also worth noting that the vector field that defines the cat map is not very regular - it is at-best of bounded variation on the flat torus. It is natural to ask: how regular can we make a vector field before it no longer mixes very well? We will return to this question later in the paper. We first go through a proof of exponential mixing to illustrate a common proof technique.

Proposition 1.7. *Correlations decay exponentially for the cat map (for sufficiently smooth observables)*

In particular, this implies that the cat map is strongly mixing and thus ergodic.

Proof. For observables $f, g \in C^\alpha(\mathbb{T}^2)$, $1/2 < \alpha \leq \infty$, we can write them as Fourier series.

$$f(x) = \sum_{n \in \mathbb{Z}^2} a_n e^{inx} \quad g(x) = \sum_{n \in \mathbb{Z}^2} b_n e^{inx}$$

We can also assume without loss of generality that f, g are mean-zero (*i.e.*, $\int_{\mathbb{T}^2} f, \int_{\mathbb{T}^2} g = 0$ which implies that $a_0, b_0 = 0$). Let A denote the matrix of the cat map. We can explicitly compute the correlation to be

$$\begin{aligned} \int_{\mathbb{T}^2} f(x)g(A^k(x))dx &= \int_{\mathbb{T}^2} \sum_{n \in \mathbb{Z}^2} a_n e^{inx} \sum_{m \in \mathbb{Z}^2} b_m e^{im \cdot A^k x} dx \\ &= \int_{\mathbb{T}^2} \sum_{n, m \in \mathbb{Z}^2} a_n b_m e^{i(n \cdot x + m \cdot A^k x)} dx \\ &= \sum_{\substack{n \in \mathbb{Z}^2 \\ n \neq 0}} a_n b_{-nA^k} \end{aligned}$$

by orthogonality. Due to the assumed regularity of f, g , we know the Fourier coefficients a_n, b_n decay like $n^{-\alpha}$. We also know that the Fourier series is absolutely convergent since $\alpha > 1/2$. Furthermore, since A is a hyperbolic matrix, we know it has one stable eigenvalue and one unstable eigenvalue (recall that an eigenvalue λ is stable if $|\lambda| < 1$ and unstable if $|\lambda| > 1$). Let λ_u denote the unstable eigenvalue (the stable eigenvalue is $1/\lambda$). Then, for any $n \in \mathbb{N}^2$,

$$\begin{aligned}\|nA^k\|^2 &= \|c_u\lambda^k v_u + c_s\lambda^{-k} v_s\|^2 \\ &= (c_u\lambda^k v_{u,1} + c_s\lambda^{-k} v_{s,1})^2 + (c_u\lambda^k v_{u,2} + c_s\lambda^{-k} v_{s,2})^2 \\ &\gg \lambda^{2k}.\end{aligned}$$

where v_u, v_s denote the unstable and stable eigenvectors and c_u, c_s the respective coefficients of n in the eigenbasis. This is because, for A , we know that the eigenvectors v_u, v_s are, respectively,

$$\left[\begin{array}{c} 1 + \sqrt{5} \\ 2 \end{array} \right] \text{ and } \left[\begin{array}{c} 1 - \sqrt{5} \\ 2 \end{array} \right],$$

so that $c_u, c_s \neq 0$ since both entries of nA^k are rational. We can then bound the correlation as follows. For large k ,

$$\begin{aligned}|C_{f,g}(k)| &= \sum_{\substack{n \in \mathbb{Z}^2 \\ n \neq 0}} a_n b_{-nA^k} \\ &\ll \sum_{\substack{n \in \mathbb{Z}^2 \\ n \neq 0}} |a_n| \|nA^k\|^{-\alpha} \\ &\ll \lambda^{-\alpha k}\end{aligned}$$

by the absolute summability of the Fourier series of a α -Hölder continuous function ($\alpha > 1/2$). \square

In particular, this proof shows that for analytic observables, the correlations decay faster than any exponential.

We can use a similar fourier analysis to show exponential decay of correlations for the tent map. However, we will use a different orthonormal basis to exploit the symmetries of the tent map.

Definition 1.8. The Haar basis is a wavelet basis consisting of “square-wave” functions. We define the “mother” wavelet as

$$H(x) = \mathbb{1}_{[0, \frac{1}{2})}(x) - \mathbb{1}_{[\frac{1}{2}, 1)}(x).$$

Then, for any $j, k \in \mathbb{N} \cup \{0\}$ with $0 \leq k \leq 2^j - 1$, we set

$$h_{j,k}(x) = 2^{j/2} H(2^j x - k).$$

This system, with the addition of the constant function $f \equiv 1$ forms an orthonormal basis for $L^2([0, 1])$. Note that $\text{supp } h_{j,k} = [k2^j, (k+1)2^j]$.

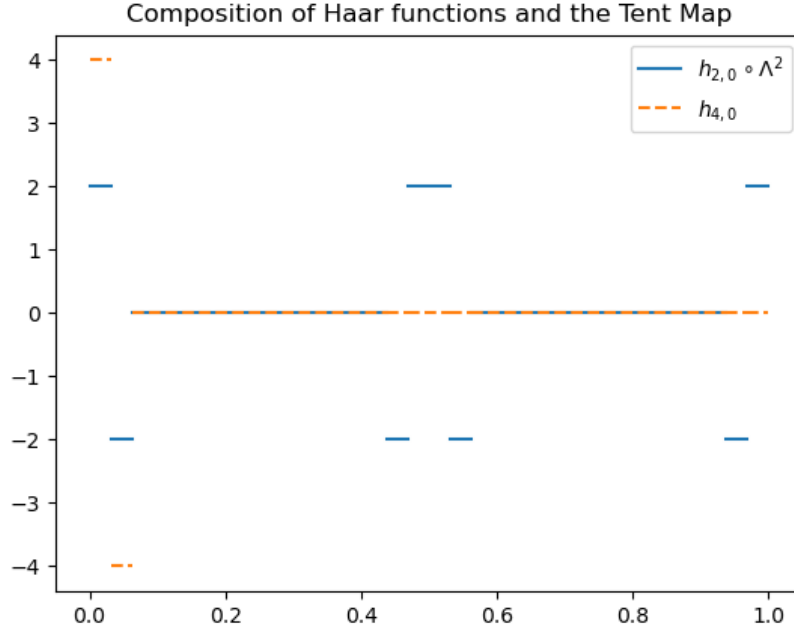


Figure 3: With appropriate rescaling and shifting, we see that we can write the blue function in terms of the orange.

Proposition 1.9. *The tent map mixes exponentially in the sense that correlations decay exponentially for all (mean-zero) continuous observables on $[0, 1]$.*

Proof. We first consider the correlations between elements of the Haar basis on $L^2([0, 1])$. In order to compute the correlations, we need to understand what the composition $h_{j,k} \circ \Lambda^n$ looks like - for our proof, we will leverage the fact that this composition can be written as a linear combination of other elements of the Haar basis (see Figure 3 for intuition).

For $j \in \mathbb{N} \cup \{0\}$, $0 \leq k \leq 2^j - 1$, we want to compute the pre-image of the sets $[k2^{-j}, (k + \frac{1}{2})2^{-j})$ and $[(k + \frac{1}{2})2^{-j}, (k + 1)2^{-j})$, which are the intervals on which $h_{j,k}$ is $2^{j/2}$ and $-2^{j/2}$, respectively. First, note that the n 'th iterate of the tent map is comprised of 2^{n-1} “tents” of slope 2^n (e.g., $\Lambda^n([0, 2^{-n}]) = [0, 1]$). Thus, we can compute that

$$\begin{aligned} & \Lambda^{-n}([k2^{-j}, (k + 1/2)2^{-j})) \\ &= \bigcup_{l=0}^{2^{n-1}-1} \left([l2^{-n+1} + k2^{-j-n}, l2^{-n+1} + (k + 1/2)2^{-j-n}) \right. \\ &\quad \left. \cup (l2^{-n+1} + 2^{-n+1} - (k + \frac{1}{2})2^{-j-n}, l2^{-n+1} + 2^{-n+1} - k2^{-j-n}] \right) \end{aligned}$$

and

$$\begin{aligned} & \Lambda^{-n}([(k + 1/2)2^{-j}, (k + 1)2^{-j})) \\ &= \bigcup_{l=0}^{2^{n-1}-1} \left([l2^{-n+1} + (k + 1/2)2^{-j-n}, l2^{-n+1} + (k + 1)2^{-j-n}) \right. \\ &\quad \left. \cup (l2^{-n+1} + 2^{-n+1} - (k + 1)2^{-j-n}, l2^{-n+1} + 2^{-n+1} - (k + 1/2)2^{-j-n}] \right) \end{aligned}$$

$$\cup (l2^{-n+1} + 2^{-n+1} - (k+1)2^{-j-n}, l2^{-n+1} + 2^{-n+1} - (k+1/2)2^{-j-n}] \Big)$$

which shows that

$$h_{j,k} \circ \Lambda^n = \sum_{l=0}^{2^{n-1}-1} 2^{-n/2} h_{j+n, k+l2^{j+1}} - 2^{-n/2} h_{j+n, (l+1)2^{j+1}-k+1}$$

So, for Haar functions $h_{j,k}$, $h_{a,b}$, by orthogonality, we know that $\int_0^1 h_{j,k} h_{a,b} dx = \delta_{ja} \delta_{kb}$. So, we can compute the correlation as follows

$$\begin{aligned} C(n) &= \int_0^1 h_{j,k}(\Lambda^n(x)) h_{a,b}(x) dx \\ &= 2^{-n/2} \sum_{l=0}^{2^{n-1}-1} \int_0^1 h_{j+n, k+l2^{j+1}}(x) h_{a,b}(x) dx \\ &\quad - 2^{-n/2} \sum_{l=0}^{2^{n-1}-1} \int_0^1 h_{j+n, (l+1)2^{j+1}-k+1}(x) h_{a,b}(x) dx \end{aligned}$$

By the previous observation about orthogonality, we know that there can at-most be *one* non-zero term because the supports of each of the elements of the sum are disjoint. Furthermore, for this non-zero term, the integral will be equal to 1, so we conclude that,

$$|C(n)| \leq 2^{-n/2}$$

for elements of the Haar basis. For general $f \in L^2([0, 1])$, we can write

$$f(x) = \sum_{j=0}^{\infty} \sum_{k=0}^{2^j-1} \langle f, h_{j,k} \rangle h_{j,k}(x),$$

and in particular, if f is continuous, the sum converges *uniformly* on $[0, 1]$ [Haa10]. We will use some enumeration of the Haar functions for more convenient notation (*i.e.*, replacing the double-indices with a single index). Then, for continuous f, g ,

$$\begin{aligned} C_{f,g}(n) &= \int_0^1 \sum_{m=0}^{\infty} \langle f, h_m \rangle h_m(\Lambda^n(x)) \sum_{l=0}^{\infty} \langle g, h_l \rangle h_l(x) dx \\ &= \sum_{m,l=0}^{\infty} \langle f, h_m \rangle \langle g, h_l \rangle \int_0^1 h_m(\Lambda^n(x)) h_l(x) dx \\ |C_{f,g}(n)| &\leq 2^{-n/2} \sum_{m,l=0}^{\infty} |\langle f, h_m \rangle| |\langle g, h_l \rangle| \\ &\leq 2^{-n/2} \left(\sum_{n=0}^{\infty} |\langle f, h_n \rangle|^2 \right)^{1/2} \left(\sum_{l=0}^{\infty} |\langle g, h_l \rangle|^2 \right)^{1/2} \\ &= 2^{-n/2} \|f\|_{L^2([0,1])} \|g\|_{L^2([0,1])} \\ &= O(2^{-n/2}) \end{aligned}$$

where we can interchange integral and sum due to uniform convergence on a compact set. \square

2 Bressan's Conjecture

This project was initially motivated by a conjecture of Alberto Bressan. Define the sets

$$\begin{aligned} A &:= \{(x_1, x_2) \in \mathbb{T}^2 \mid 0 \leq x_1 < 1/2\} \\ A' &:= \{(x_1, x_2) \in \mathbb{T}^2 \mid 1/2 \leq x_1 < 1\} \end{aligned}$$

Conjecture 2.1 ([Bre03]). There exists a constant $\beta > 0$ such that the following holds. For any $\varepsilon \in (0, 1/4]$ and $T > 0$, if $f : [0, T] \times \mathbb{T}^2 \rightarrow \mathbb{R}^2$ is a smooth, divergence-free vector field on \mathbb{T}^2 whose flow mixes the sets A, A' up to scale ε , then

$$\int_0^T \int_{\mathbb{T}^2} \|\nabla_x f(t, x)\|_1 dx dt \geq \beta |\log \varepsilon|$$

This conjecture has been resolved in the setting where the L^1 norm is replaced by L^p for $p > 1$ [CDL08] via the theory of renormalized solutions. In other words, it is true that for any $p > 1$, there exists some constant $C > 0$ independent of ε such that,

$$\int_0^T \int_{\mathbb{T}^2} \|\nabla_x f(t, x)\|_{L^p} dx dt \geq C |\log \varepsilon|.$$

Even more recently, another method of resolving the conjecture in the $p > 1$ case was provided in [Lég18] using harmonic analysis estimates. Unfortunately, it seems like neither of these methods can effectively deal with the L^1 case.

While Bressan's conjecture focuses on the work needed to mix effectively, there is also the “dual” question of what do such mixing flows look like? For example, given a constraint on the regularity of the vector field, can we still find a flow that mixes exponentially? As mentioned in the discussion on dynamical systems, the flow that generates the cat map is only of bounded variation. In [EZ19], they show the existence of α -Hölder ($\alpha < 1$) vector fields that mix exponentially. One question we will examine in this paper is that of whether there exists a Lipschitz vector field that also mixes exponentially.

In particular, we start with the candidate vector field

$$\mathfrak{f}(t, x_1, x_2) = \begin{cases} (\Lambda(x_2), 0) & t \in [2n, 2n+1) \\ (0, \Lambda(x_1)) & t \in [2n+1, 2n+2) \end{cases} \quad (2.1)$$

for $n \in \mathbb{N} \cup \{0\}$, which can be thought of as a modification of the cat map to make it continuous (we will often refer to the map defined by this flow as the continuous cat map). Λ is the tent map as defined earlier. This flow is comprised of alternating horizontal and vertical shears like that of the cat map but is continuous at the boundaries of the unit square with opposite edges identified (see Figure 4). We will use \mathfrak{F} to denote the map induced by \mathfrak{f} over two integer time-steps, *i.e.*,

$$\mathfrak{F}(x_1, x_2) = (x_1 + \Lambda(x_2), x_2 + \Lambda(x_1 + \Lambda(x_2))). \quad (2.2)$$

Unforunately, we will soon see that this flow is in fact a *very poor* mixer. However, not all hope is lost as we will also soon see that there are very similar flows which mix rather well.

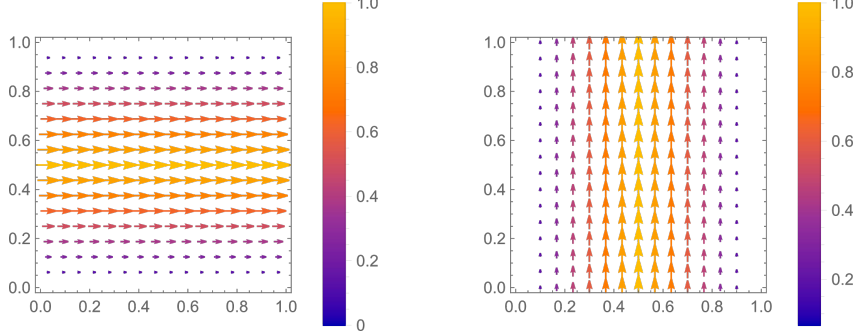


Figure 4: The alternating shears of \mathfrak{F} .

3 Building Intuition with Simulations

In this section we present and discuss various plots of mixing. For example, we will look at what happens to certain scalar functions advected by our flow. Of note is a very recent paper on arXiv that numerically studies the same flows we consider and presents numerical evidence that such alternating horizontal and vertical shears are exponential mixers [CRWZ21]. These plots will help us develop our intuition regarding the mixing properties of these *alternating wedge flows*. We will use this term to refer to the family of vector fields (and their induced maps) we define below.

In the previous section, we defined the map \mathfrak{F} (2.2) in terms of the tent map; however, we can alternatively write this map as the composition $(V_2 \circ H_2)$ where we define

$$w_k(z) = -k|z - 1/2| \pmod{1} \quad (3.1)$$

and

$$H_k(x, y) = (x + w_k(y), y) \pmod{1}, \quad V_k(x, y) = (x, y + w_k(x)) \pmod{1}. \quad (3.2)$$

This formulation allows us to generalize our previous flow and can be interpreted as modifying the time we allot to the horizontal and vertical shears before switching to the other direction. In Figure 5 we plot the images of the set $A = \{(x, y) \in \mathbb{T}^2 \mid 0 \leq x < 1/2\}$ under these alternating wedge flows.

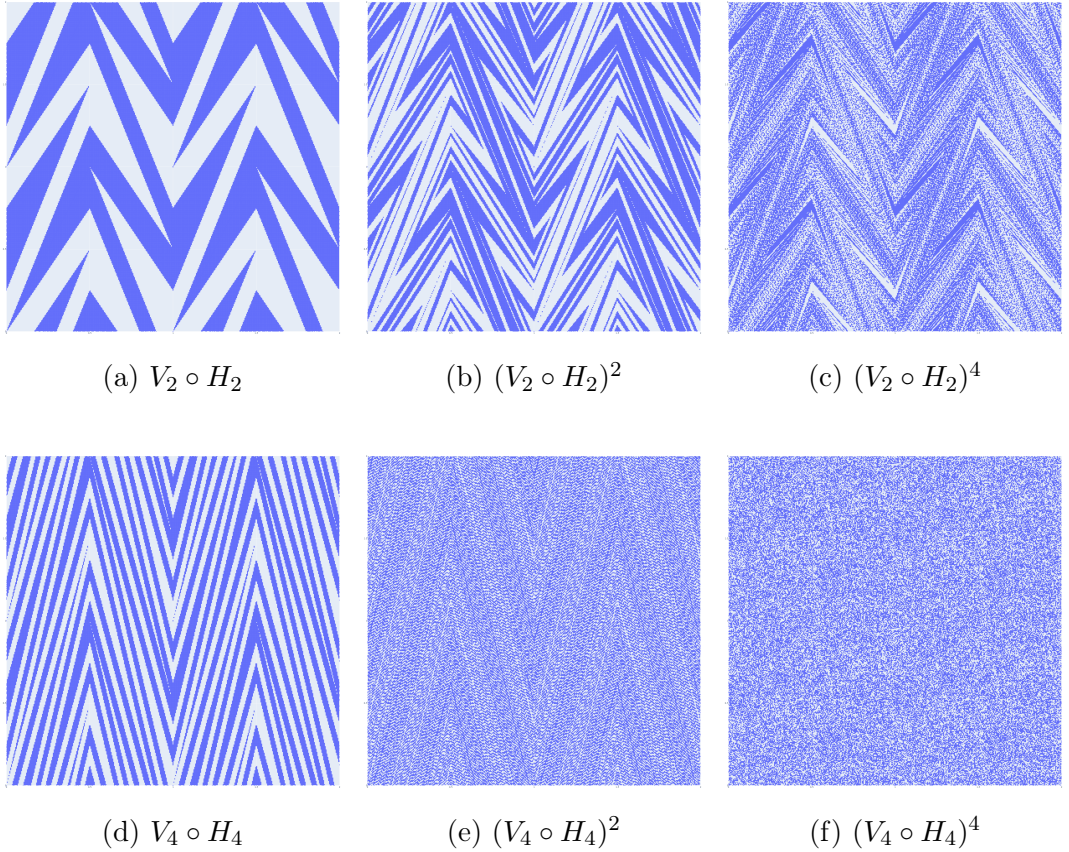


Figure 5: In each image, 4 copies of the unit square are tiled following the periodic boundary conditions that define the torus.

In [CRWZ21], they provide numerical evidence indicating that the flows corresponding to $k > 2$ are exponential mixers; however, that when $k = 2$ there can be at-best algebraic mixing. Some visual evidence for this can be seen in the right-most images of Figure 5. In the plot of $(V_2 \circ H_2)^4$, there appear to be rectangular strips of solid white and solid blue which represent unmixed regions. In Figure 6 we see that the trajectory of a point very near one of these unmixed regions stays close for a while but eventually escapes.

We study the properties of \mathfrak{F} and other flows belonging to the family $(V_K \circ H_K)$ in greater detail in the following section.

4 Properties of the Alternating Wedge Flows

Throughout this section, \mathfrak{f} and \mathfrak{F} denote the flow and corresponding map defined in (2.1) and (2.2). We will focus on the maps corresponding to $K = 2$ and $K = 4$. In particular, we will also focus our attention to a dense subset of the points in $[0, 1]^2$ – namely, the dyadic rationals. One property we immediately notice is that these dyadic rationals are periodic under our family of maps.

Definition 4.1. Let $D_m := \{(i2^{-m}, j2^{-m}) \in \mathbb{T}^2 \mid i, j \text{ odd}\}$ denote the set of irreducible dyadic rationals with denominator $m \in \mathbb{N}$. We define the dyadic rationals as the set $D = \bigcup_{m=1}^{\infty} D_m$.

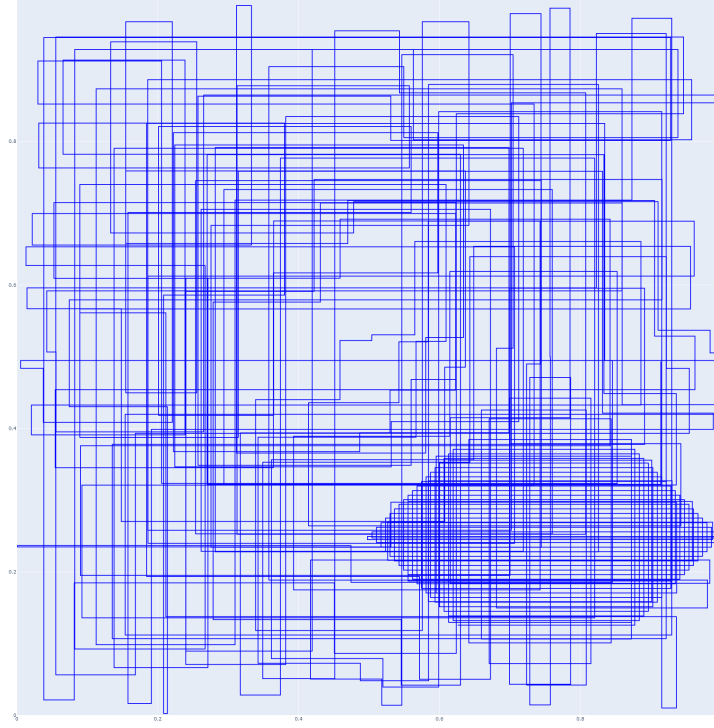


Figure 6: 500 steps of the trajectory of $(\frac{5}{8} + 8 \times 10^{-4}, \frac{1}{8} + 8 \times 10^{-4})$.

Proposition 4.2. *For $K \in \mathbb{N}$, every dyadic rational is periodic under the map $(V_K \circ H_K)$.*

Proof. Recall that

$$H_K(x, y) = (x + w_K(y), y) \pmod{1} \quad \text{and} \quad V_K(x, y) = (x, y + w_K(x)) \pmod{1},$$

where

$$w_K(z) = -K|z - 1/2| \pmod{1}.$$

The first step is to notice that the denominator of a dyadic point does not increase under iterations of the map. For any $(i2^{-m}, j2^{-m})$, $i, j = 0, \dots, 2^m - 1$, we just need to show that $w_k(x)$ and $w_k(x + w_k(y))$ don't have a larger denominator than 2^m .

$$\begin{aligned} w_K(i2^{-m}) &= -K|(i - 2^{m-1})2^{-m}| \pmod{1} \\ &= \frac{-K}{2^m}|i - 2^{m-1}| \pmod{1} \end{aligned}$$

and now it is clear that the numerator is some integer so that, if $w_k(i2^{-m})$ is non-zero, it must be at least 2^{-m} .

Now, by pigeonhole principle, after $2^m + 1$ iterations, one of the dyadic points with denominator 2^{-m} must have been visited twice.

The last step is to show that this point must be the same as the starting point. In other words, our starting point does not get sucked into the orbit of another point. This property follows rather immediately from the fact that the map $(V_K \circ H_K)$ is invertible so that no point can have more than one pre-image. \square

4.1 The Continuous Cat Map ($V_2 \circ H_2$)

We now shift our focus to the claim of algebraic mixing in [CRWZ21] which they do not prove. In particular, this would imply that the flow \mathfrak{f} is *not* an exponential mixer. This is not the end of the world, though, as it seems like slightly faster flows (such as that corresponding to $V_4 \circ H_4$) are indeed exponential mixers. The unmixed regions in subplot (c) of Figure 5 correspond to neighborhoods of the (open) line segments

$$\begin{aligned}s_1 &:= \{(1/2 + t, 1/4 - t) \mid t \in (0, 1/4)\}, \\ s_2 &:= \{(3/4 + t, 1/2 - t) \mid t \in (0, 1/4)\}, \\ s_3 &:= \{(1/4 + t, 1/2 + t) \mid t \in (0, 1/4)\}, \\ s_4 &:= \{(0 + t, 3/4 + t) \mid t \in (0, 1/4)\}.\end{aligned}$$

The line segments s_1 and s_2 are mapped to each other by \mathfrak{F} (and similarly for s_3 and s_4), so for a point on the line segment s_2 (or s_1), we can explicitly calculate what \mathfrak{F} looks like. To be more precise, s_1 is mapped to the reverse of s_2 (*i.e.*, the point on s_1 corresponding to $t = s$ is mapped to the point on s_2 corresponding to $t = 1/4 - s$). Being careful about where these points lie in the domain of the tent map Λ , we can write that for $(x, y) \in s_1 \cup s_2$,

$$\begin{aligned}\mathfrak{F}(x, y) &= (x + \Lambda(y), y + \Lambda(x + \Lambda(y))) \pmod{1} \\ &= (x + 2y, y + \Lambda(x + 2y)) \pmod{1} \\ &= (x + 2y, y + 2 - 2(x + 2y)) \pmod{1}.\end{aligned}$$

Thus, on s_1 and s_2 , the map \mathfrak{F} can be represented by the matrix

$$A = \begin{bmatrix} 1 & 2 \\ -2 & -3 \end{bmatrix},$$

and similarly, on s_3 and s_4 ,

$$B = \begin{bmatrix} 1 & -2 \\ 2 & -3 \end{bmatrix}.$$

Both of these matrices are similar to 2×2 Jordan blocks with -1 on the diagonal and both have only $(-1, 1)$ or $(1, 1)$ as their eigenvector, respectively. As a quick check, we note that these vectors agree with the directions of their corresponding lines. Furthermore, we see that s_1 and s_2 are fixed by A^2 and similarly for s_3 and s_4 by B^2 . With this perspective, we can show that near any point on these lines, mixing only occurs at a rate of n^{-1} .

For simplicity, we will focus our attention to points near s_1 . We can explicitly compute the Jordan canonical form of A^2 to be

$$A^2 = \begin{bmatrix} -1 & \frac{1}{4} \\ 1 & 0 \end{bmatrix} \begin{bmatrix} 1 & 1 \\ 0 & 1 \end{bmatrix} \begin{bmatrix} 0 & 1 \\ 4 & 4 \end{bmatrix}.$$

Take $x \in s_1$ and let $\delta = [\delta_1, \delta_2]^T$ be a small perturbation vector such that $\delta_1 \neq -\delta_2$ (*i.e.*, so that $x + \delta \notin s_1$). Then,

$$(A^2)^n(x + \delta) = x + A^{2n}\delta$$

$$\begin{aligned}
&= x + \begin{bmatrix} (1-4n)\delta_1 - 4n\delta_2 \\ 4n\delta_1 + (1+4n)\delta_2 \end{bmatrix} \\
&= x + \delta + 4n(\delta_1 + \delta_2) \begin{bmatrix} -1 \\ 1 \end{bmatrix},
\end{aligned}$$

which shows that points near s_1 move away from it at a linear rate rather than exponentially quickly. In particular, we can use this to show that the functional mixing scale decays at most linearly in time. By a kind of “interpolation” inequality (which follows from applying Cauchy-Schwarz to the Fourier definition of the \dot{H}^k norms - note that $L^2 = H^0$), we get the following bound on the \dot{H}^{-1} norm.

$$\|\varrho(\cdot, t)\|_{L^2}^2 \leq \|\varrho(\cdot, t)\|_{\dot{H}^1} \|\varrho(\cdot, t)\|_{\dot{H}^{-1}} \implies \|\varrho(\cdot, t)\|_{\dot{H}^{-1}} \geq \frac{\|\varrho(\cdot, t)\|_{L^2}^2}{\|\varrho(\cdot, t)\|_{\dot{H}^1}}$$

In particular, we can apply this to a subset of the domain; the subset we are interested in will be a neighborhood of the line s_1 . We can then upper bound the H^1 norm using our $x + \delta$ calculation from above and we know the L^2 norm of ϱ is conserved by the transport equation (see (1.5), Section 1.2). The $x + \delta$ calculation gives us a bound on the derivative of our map $(V_2 \circ H_2) = \mathfrak{F}$ which locally behaves like the matrix A . Explicitly, near the lines s_1 and s_2 , for $\delta \in \mathbb{R}^2$, $\delta_1 + \delta_2 \neq 0$,

$$\begin{aligned}
\nabla \mathfrak{F}^{2n}(\mathbf{x}) &= \lim_{\delta \rightarrow 0} \frac{\mathfrak{F}^{2n}(\mathbf{x} + \delta) - \mathfrak{F}^{2n}(\mathbf{x})}{\|\delta\|} \\
&= \lim_{\delta \rightarrow 0} \frac{(A^2)^n(\mathbf{x} + \delta) - \mathbf{x}}{\|\delta\|} \\
&= \lim_{\delta \rightarrow 0} \frac{1}{\|\delta\|} \begin{bmatrix} \delta_1 - 4n(\delta_1 + \delta_2) \\ \delta_2 + 4n(\delta_1 + \delta_2) \end{bmatrix} \\
\|\nabla \mathfrak{F}^{2n}(\mathbf{x})\| &\ll |n|
\end{aligned}$$

Then, on this subset, we can upper bound the \dot{H}^1 norm using chain rule.

$$\begin{aligned}
\|\varrho(\cdot, 2n)\|_{\dot{H}^1} &= \|\varrho(\mathfrak{F}^{-2n}(\cdot), 0)\|_{\dot{H}^1} \\
&= \|\nabla \varrho(A^{-2n}(\cdot), 0)\|_{L^2} \\
&\leq \|(\nabla \varrho)(A^{-2n}(\cdot), 0)\| \|\nabla A^{-2n}\|_{L^\infty} \\
&\ll n
\end{aligned}$$

where we can assume sufficient regularity of the initial datum $\varrho(\cdot, 0)$ such that the gradient is uniformly bounded. Now, this implies that

$$\|\varrho(\cdot, 2n)\|_{\dot{H}^{-1}} \gg n^{-1}$$

which implies that $\mathfrak{F} = (V_2 \circ H_2)$ is at-best an algebraic mixer.

4.2 Properties of $(V_4 \circ H_4)$

Like the beginning of this section, we start by examining the period of the dyadic rationals. Towards proving exponential mixing, we would like to show that the period

of a point $(i2^{-m}, j2^{-m})$, i, j odd numbers, grows linearly in m . To contrast this with the map studied in the previous section, we see that the minimum period of such points is constant for $m \geq 2$ because we can always find a such a point on one of the lines s_1, s_2, s_3, s_4 . In Figure 7, we see the difference between the periods of the dyadic points (up to 2^{-8}) under iterations of the maps $(V_2 \circ H_2)$ and $(V_4 \circ H_4)$.

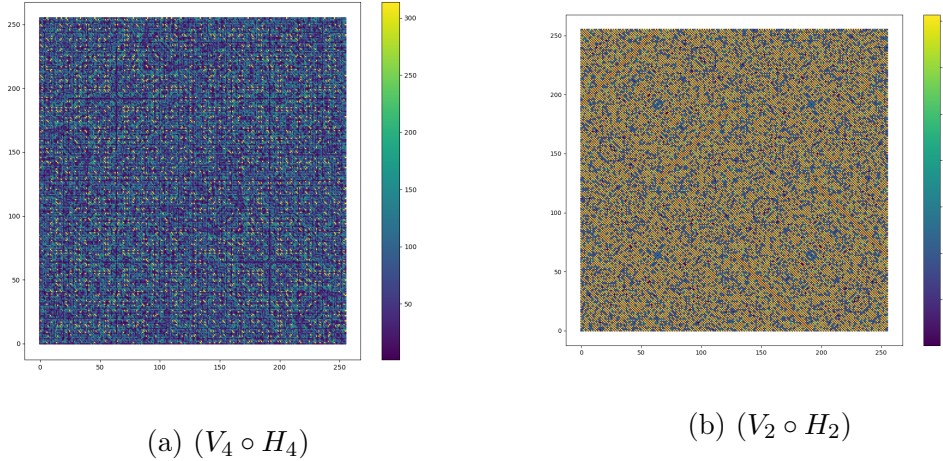


Figure 7: Period of all dyadic points up to 2^{-8} under alternating wedge flows.

To further motivate the idea that the period grows linearly in the exponent, we have numerically determined the period of the points belonging to D_m up to $m = 20$.

m	min period						
1	1	6	4	11	6	16	16
2	1	7	4	12	6	17	10
3	2	8	10	13	10	18	16
4	2	9	6	14	14	19	18
5	4	10	6	15	14	20	16

Table 1: Minimum period is defined as $\min_{x \in D_m} \text{period}(x)$.

Theorem 4.3. Suppose the point $(i2^{-m}, j2^{-m})$, i, j odd integers, has period N under the map $(V_4 \circ H_4)$, then $m \leq 4N$.

Proof. Recall that $H_4(x, y) = (x + w_4(y), y) \pmod{1}$ and $V_4(x, y) = (x, y + w_4(x)) \pmod{1}$ where

$$w_4(z) = -4|z - 1/2| \pmod{1} = \begin{cases} 4z & z \in [0, 1/4) \\ 4z - 1 & z \in [1/4, 1/2) \\ -4z + 3 & z \in [1/2, 3/4) \\ -4z + 4 & z \in [3/4, 1] \end{cases}.$$

The first step is to notice that

$$w_4(z) \equiv \pm 4z \pmod{1}.$$

This form will allow us to study compositions of w_4 more easily. We will use the shorthand $w = w_4$ from here on out. For example,

$$w(x + w(y)) \equiv \pm 4x \pm 16y \pmod{1}.$$

Next, we recall that if a point has period N , then $(V_4 \circ H_4)^N(x, y) = (x, y)$.

To introduce the strategy we will use, we start with the case where $N = 2$. We can write the second-iterate of (x, y) as

$$\begin{aligned} (V_4 \circ H_4)^2(x, y) &= (x + w(y) + w(y + w(x + w(y)))), \\ &\quad y + w(x + w(y)) + w(x + w(y) + w(y + w(x + w(y))))), \end{aligned}$$

where we suppose that at least one of $w(y)$ and $w(x + w(y))$ is not an integer (otherwise the point would have period 1). Period 2 implies that

$$\begin{aligned} \eta &:= w(y) + w(y + w(x + w(y))) \in \mathbb{Z}, \\ \zeta &:= w(x + w(y)) + w(x + \eta) \in \mathbb{Z}. \end{aligned}$$

In fact, since $\eta \in \mathbb{Z}$, we know that $w(x + \eta) = w(x)$ so that $w(x + w(y)) + w(x) \in \mathbb{Z}$. Now, using the expression for $w(x) \pmod{1}$, for $(x, y) = (i2^{-m}, j2^{-m}) \in D_m$ we can write

$$\begin{aligned} 0 &\equiv w(x + w(y)) + w(x) \pmod{1} \\ &\equiv \pm 4x \pm 4(x \pm 4y) \pmod{1} \\ &\equiv \pm i2^{-m+2} \pm i2^{-m+2} \pm j2^{-m+4} \pmod{1} \end{aligned}$$

but since i, j are odd, for this expression to be an integer, it must be the case that $4 - m \geq 0$ which implies that $m \leq 4$.

For the case of general $N \in \mathbb{N}$, we notice that

$$\begin{aligned} (V_4 \circ H_4)(x, y) &= (x + w(y)_1, \\ &\quad y + w(x + w(y)_1)_2), \\ (V_4 \circ H_4)^2(x, y) &= (x + w(y) + w(y + w(x + w(y)_1)_2)_3, \\ &\quad y + w(x + w(y)) + w(x + w(y) + w(y + w(x + w(y)_1)_2)_3)_4), \end{aligned}$$

where the subscripts are to make clear the number of compositions. In other words, we see that amongst all terms in the y component of $(V_4 \circ H_4)^N(x, y)$, the maximum possible number of nested w 's will be $2N$ (which follow from an induction argument). Thus, we see that if (x, y) is N -periodic, there is, in the worst-case, a $2N$ -fold composition of w that must result in an integer. That is, in the worst case we have

$$\pm 4^{2N}y \equiv 0 \pmod{1},$$

which implies that $4N - m \geq 0$. \square

There are a few details in this proof that remain to be fully worked out, such as the claim that the odd numerators prevent us from forming integers with points who have denominator larger than $2N$, which will be addressed during the following semester.

Remark 4.4. We note that the bound above may not be sharp, we believe that the constant can be improved from 4 to 2 by more careful analysis about how many compositions of w actually occur. As we see in the case with $N = 2$, there is a lot of cancellation. For example, we know that the term of the y -component which comes from V_4 can be reduced to $w(x)$ by the periodicity assumption.

5 Discussion and Conclusion

In this essay, we have introduced various quantitative measures of mixing and discussed their interrelationship. We then introduce an unsolved conjecture about how much “work” a vector field must do to mix a certain initial condition, and inspired by this conjecture, we discuss the “dual” problem which studies the properties of these mixing vector fields. We focus on the regularity problem where we challenge ourselves to find a Lipschitz vector field that still mixes exponentially.

To answer this problem, we introduce a family of Lipschitz vector fields and identify specific candidates for exponential mixing. We show that one of these candidates is at-best an algebraic mixer and we show that the period of the dyadic rationals under the other candidate grows linearly in the exponent of the denominator. Throughout the essay, we also provide many numerical examples to help build our intuition about the way in which these vector fields mix.

Future Work: For this specific problem, we hope to use our result lower-bounding the period of the dyadic rationals to prove exponential mixing during the coming semester. There are also other interesting directions for future work:

- Is Lipschitz the most regular we can go? The next step could be to consider $C^{1,\alpha}$ vector fields for $\alpha \in [0, 1)$.
- Of course, one can also work towards resolving Bressan’s conjecture, though this direction of work will likely require very different mathematics from what is used in this essay.
- Lastly, one can study mixing on other domains, such as the unit cube. After all, the torus is not a physically relevant domain and instead one should consider bounded subsets of \mathbb{R}^3 if one is interested in physically relevant mixing results.

References

- [Bre03] Alberto Bressan. A lemma and a conjecture on the cost of rearrangements. *Rendiconti del Seminario Matematico della Universita di Padova*, 110:97–102, 2003.
- [CDL08] Gianluca Crippa and Camillo De Lellis. Estimates and regularity results for the diperna-lions flow. 2008.
- [CRWZ21] Li-Tien Cheng, Frederick Rajasekaran, Kin Yau James Wong, and Andrej Zlatoš. Numerical evidence of exponential mixing by alternating shear flows, 2021.
- [EZ19] Tarek M Elgindi and Andrej Zlatoš. Universal mixers in all dimensions. *Advances in Mathematics*, 356:106807, 2019.
- [Haa10] A. Haar. Zur theorie der orthogonalen funktionensysteme. (erste mitteilung). *Mathematische Annalen*, 69:331–371, 1910.

- [Lég18] Flavien Léger. A new approach to bounds on mixing. *Mathematical Models and Methods in Applied Sciences*, 28(05):829–849, 2018.
- [LLN⁺12] Evelyn Lunasin, Zhi Lin, Alexei Novikov, Anna Mazzucato, and Charles R. Doering. Optimal mixing and optimal stirring for fixed energy, fixed power, or fixed palenstrophy flows. *Journal of Mathematical Physics*, 53(11), November 2012.
- [MMP05] George Mathew, Igor Mezić, and Linda Petzold. A multiscale measure for mixing. *Physica D: Nonlinear Phenomena*, 211(1):23–46, 2005.
- [OTD20] Bryan W. Oakley, Jean-Luc Thiffeault, and Charles R. Doering. On mix-norms and the rate of decay of correlations, 2020.
- [Thi12] Jean-Luc Thiffeault. Using multiscale norms to quantify mixing and transport. *Nonlinearity*, 25(2):R1, 2012.